

Supplementary material

Simultaneous inhibition of heat shock proteins and autophagy enhances radiofrequency ablation of hepatocellular carcinoma

Jinchao Zhao,^a Lei Lei,^a Wenbin Dai,^b Angfeng Jiang,^a Qiao Jin,^{*,b} and Zhe Tang,^{*,a,c}

^a Department of General Surgery, The Fourth Affiliated Hospital, International Institutes of Medicine, Zhejiang University School of Medicine, Yiwu, 322000, China.

^b MOE Key Laboratory of Macromolecular Synthesis and Functionalization, Department of Polymer Science and Engineering, Zhejiang University, Hangzhou, 310058, China.

^c Department of Surgery, The Second Affiliated Hospital, Zhejiang University School of Medicine, Hangzhou, 310009, China.

Corresponding author:

*E-mail: jinqiao@zju.edu.cn (Q. J.), 8xi@zju.edu.cn (Z.T.)

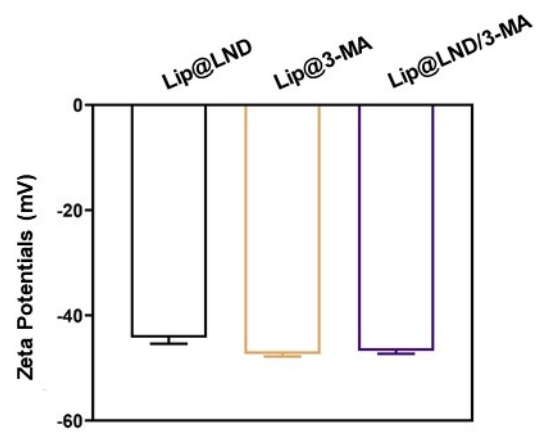


Figure S1. The zeta potentials of Lip@LND, Lip@3-MA and Lip@LND/3-MA (n=3).

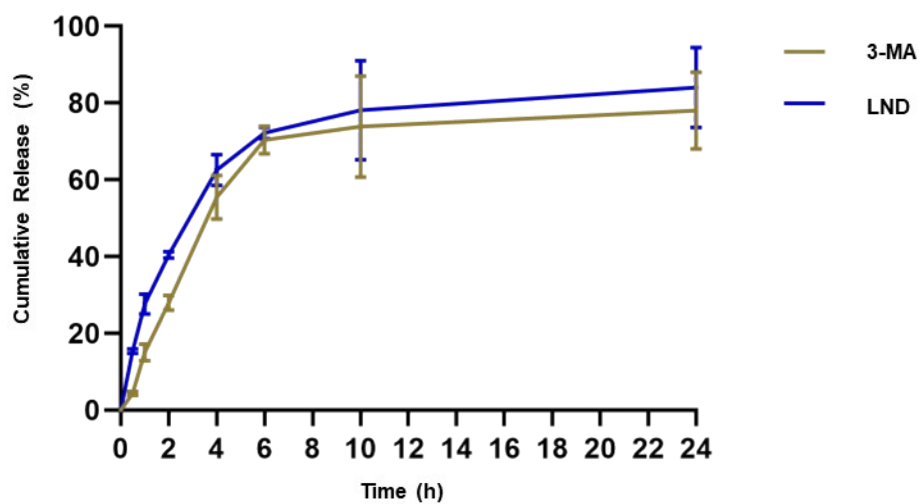


Figure S2. The cumulative release of Lip@LND/3-MA *in vitro* (n=3).

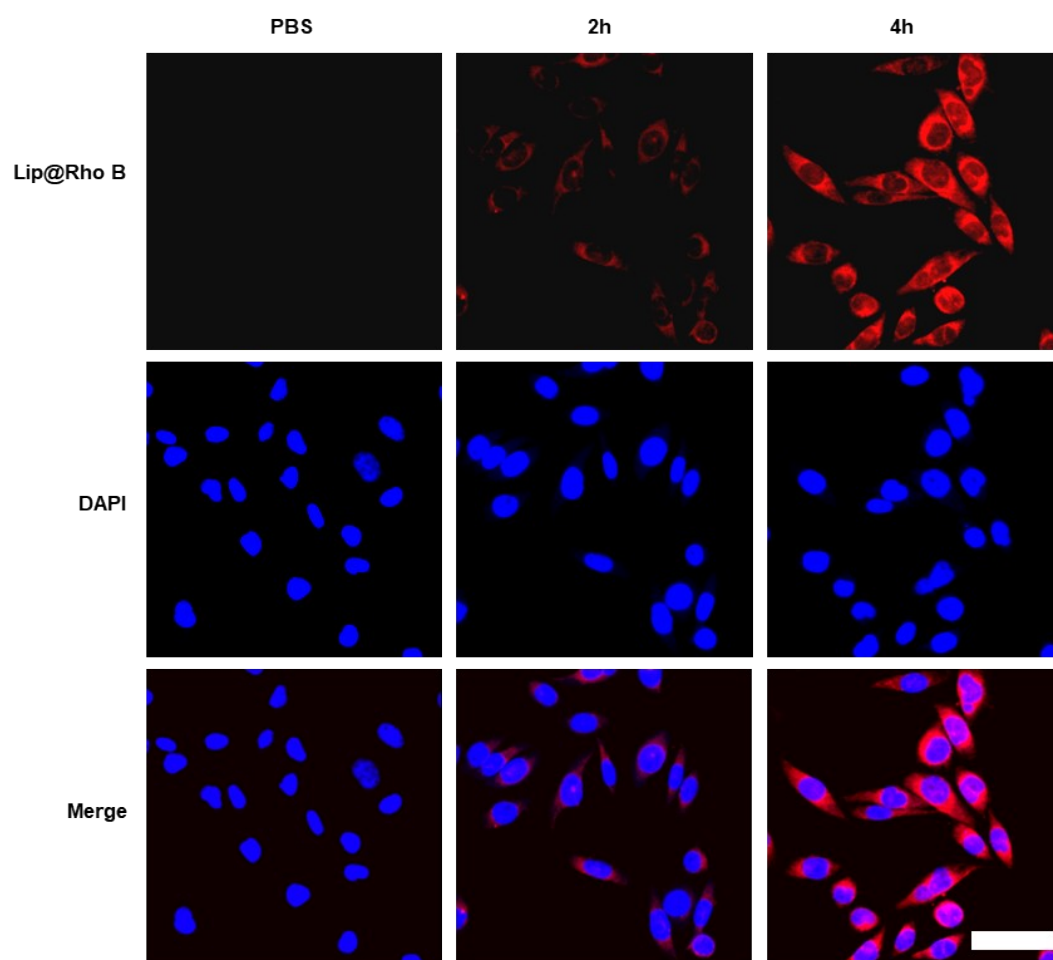


Figure S3. The cellular uptake of Lip@Rho B by LM3 cells *in vitro*. Scale bar: 20 μm .

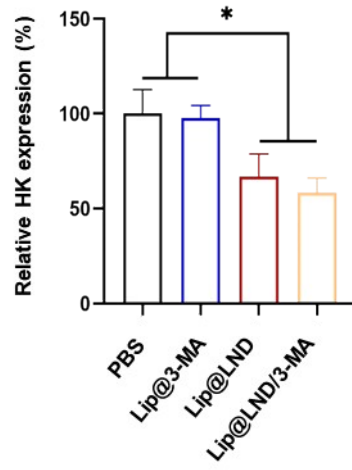


Figure S4. The relative hexokinase expression measured by western blot.

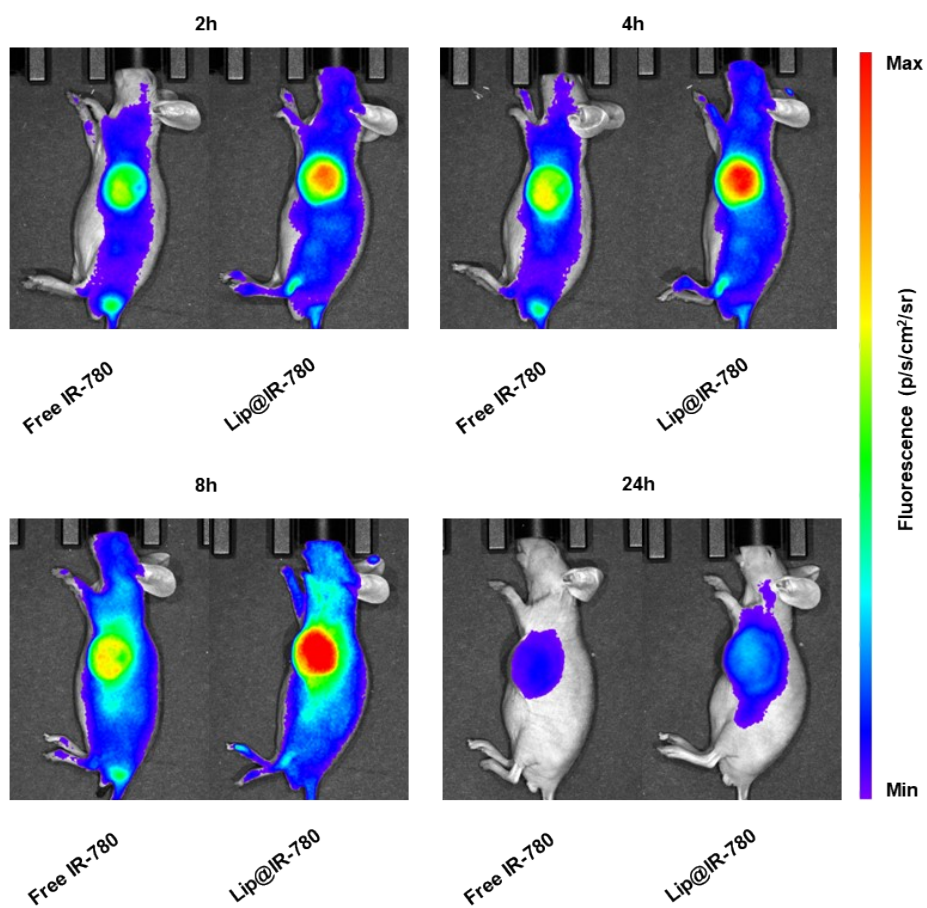


Figure S5. The body imaging of Lip@IR-780 in the LM3 tumor model at different time interval.

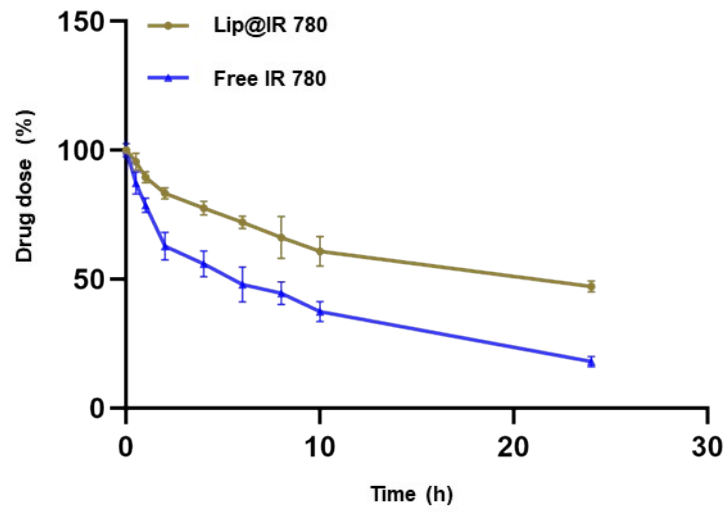


Figure S6. The pharmacokinetics of Lip@IR-780 in the LM3 tumor model *in vivo* (n=3).

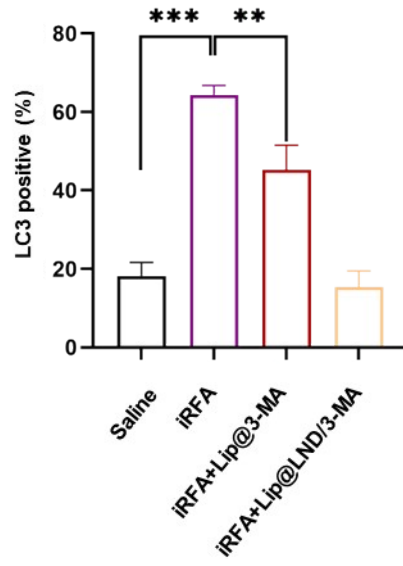


Figure S7. The LC3 positive rate after different treatments (n=3).

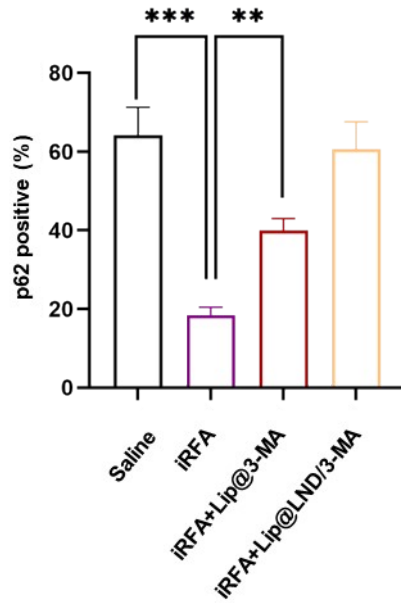


Figure S8. The p62 positive rate after different treatments (n=3).

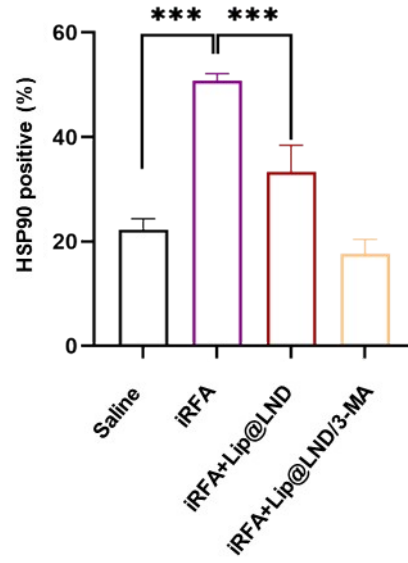


Figure S9. The HSP90 positive rate after different treatments (n=3).

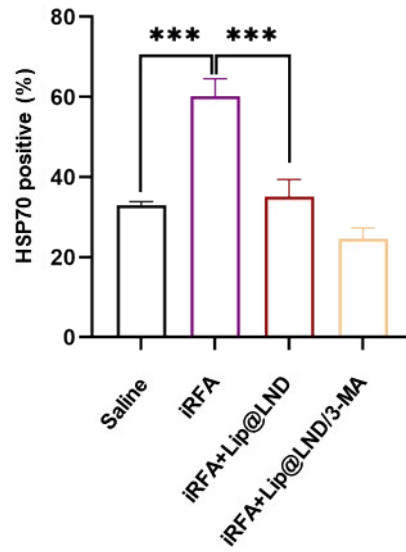


Figure S10. The HSP70 positive rate after different treatments (n=3).

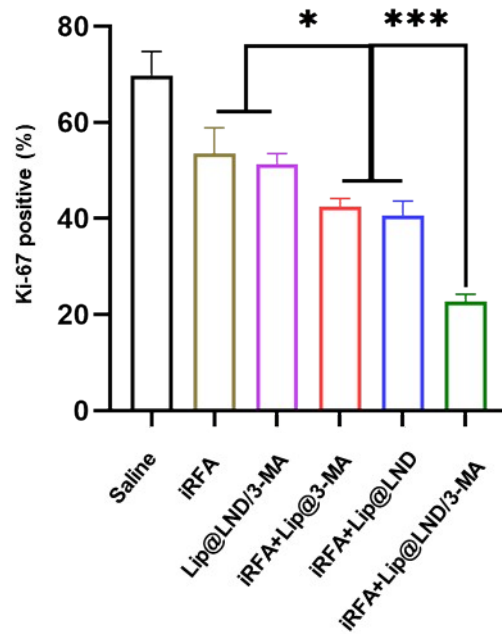


Figure S11. The Ki-67 positive rate after different treatments (n=3).

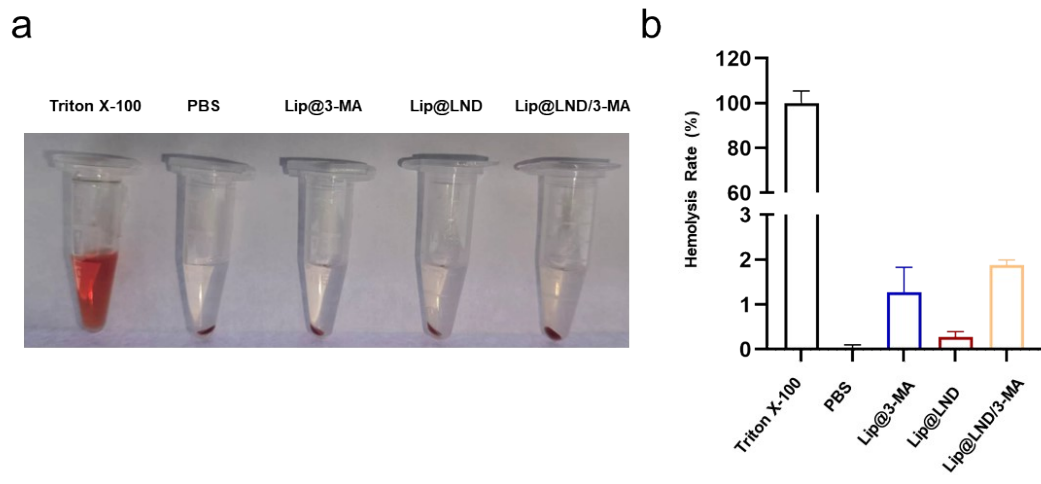


Figure S12. The photograph of hemolysis (a) and the hemolysis rate (b) after different treatments (n=3).

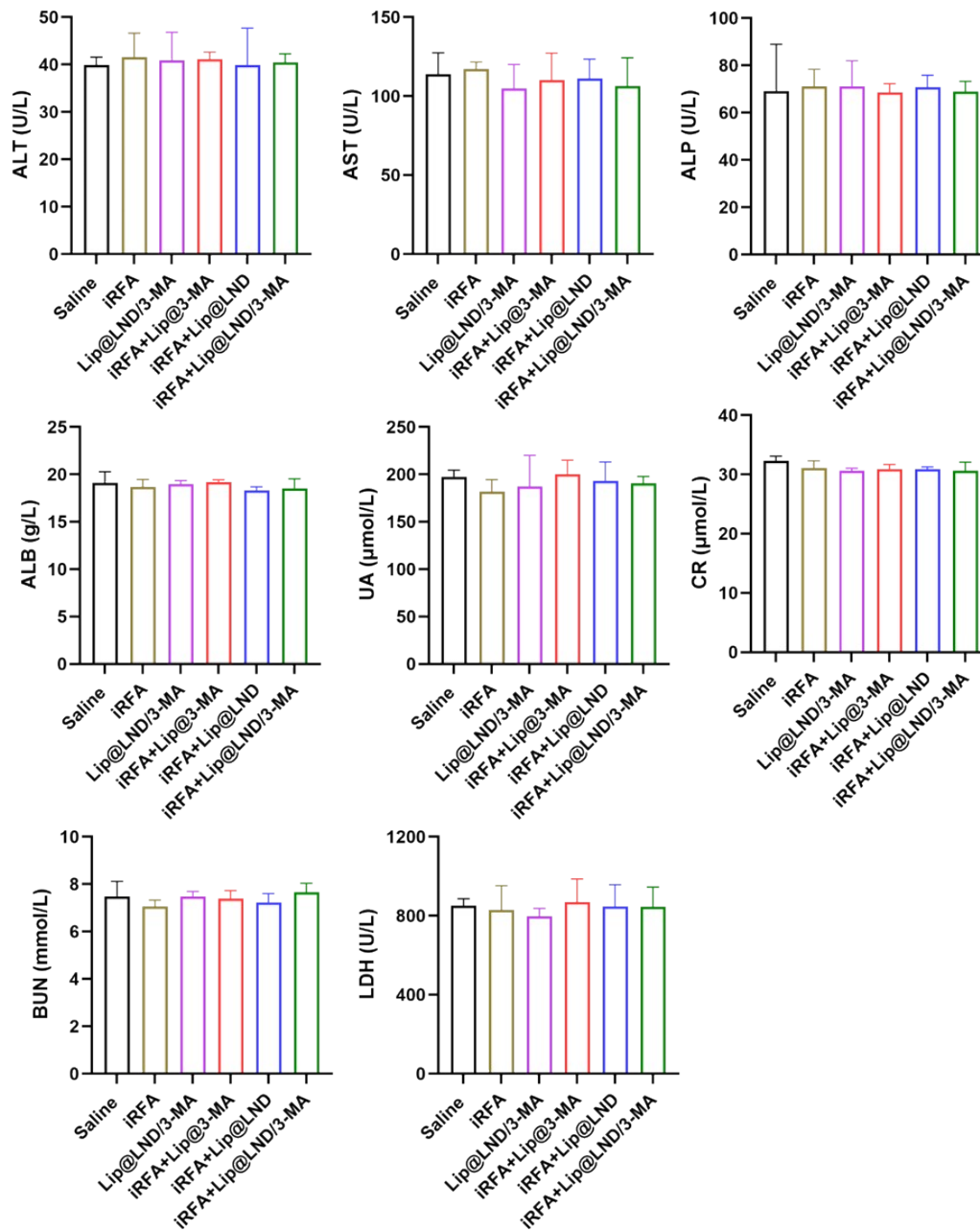


Figure S13. The blood biochemistry results in LM3 tumor model after different treatments (n=3).

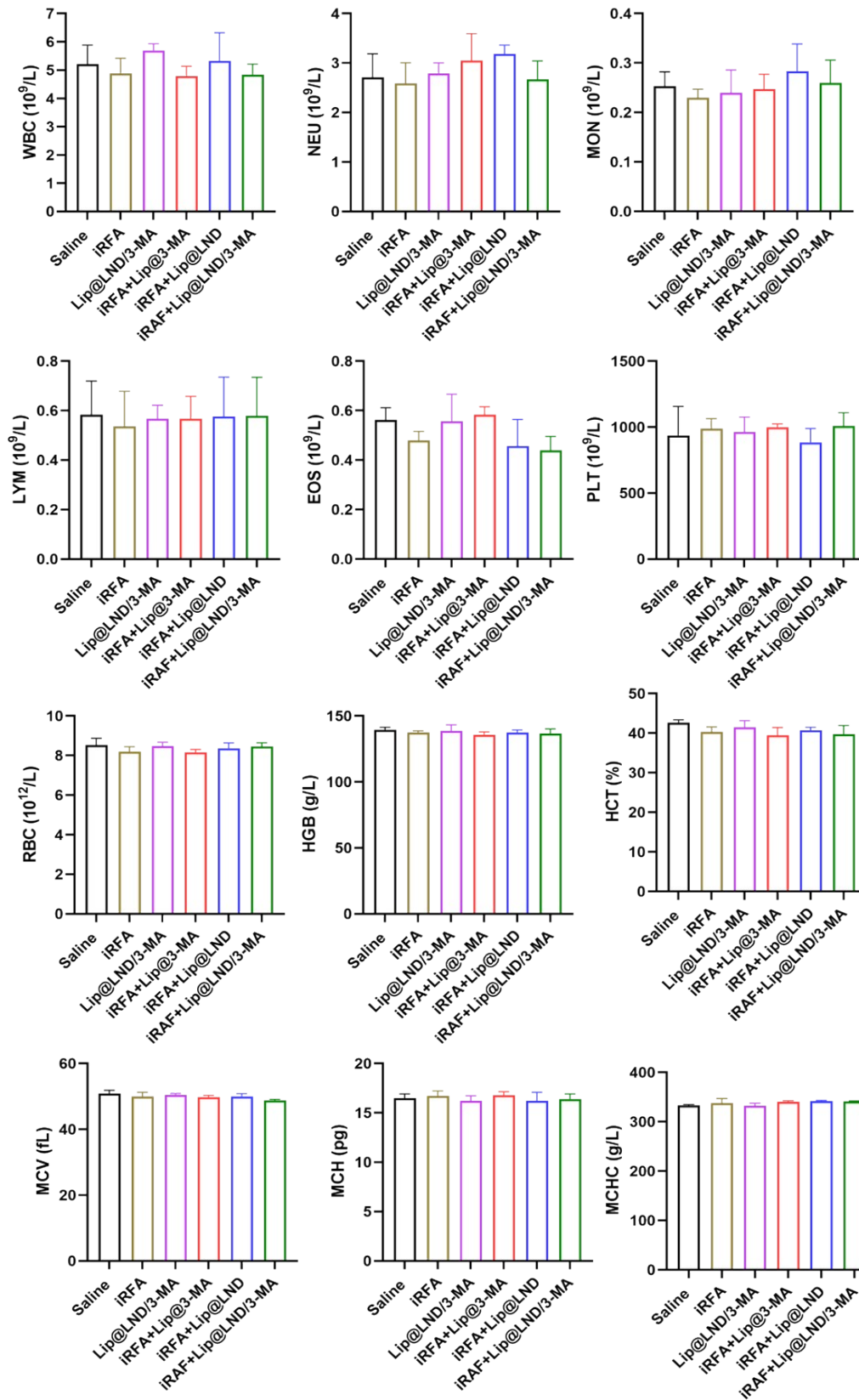


Figure S14. The blood routine results in LM3 tumor model after different treatments

(n=3).

Table S1. The encapsulation rate (ER) and drug loading content (DLC).

Sample	ER (%)		DLC (%)	
	3-MA	LND	3-MA	LND
/	3-MA	LND	3-MA	LND
Lip@3-MA	88.84	/	2.56	/
Lip@LND	/	86.82	/	3.29
Lip@LND/3-MA	86.92	85.00	1.28	2.9

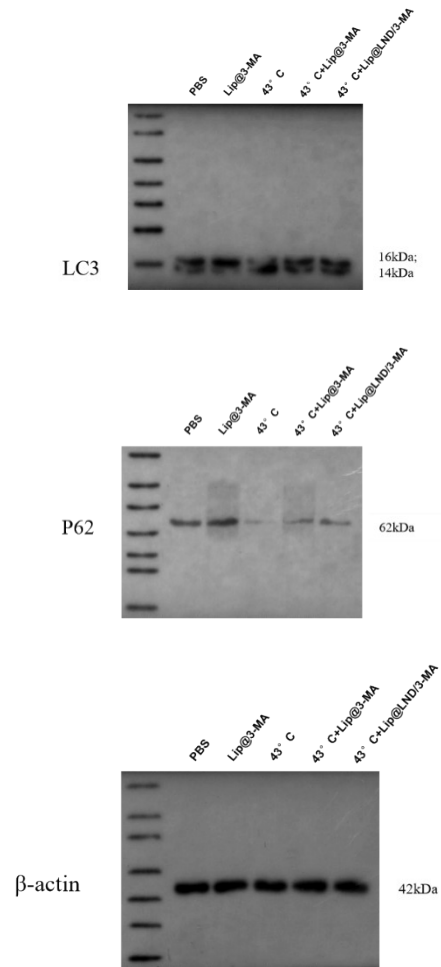


Figure S15. The image of the full gel and blot for Fig 2a.

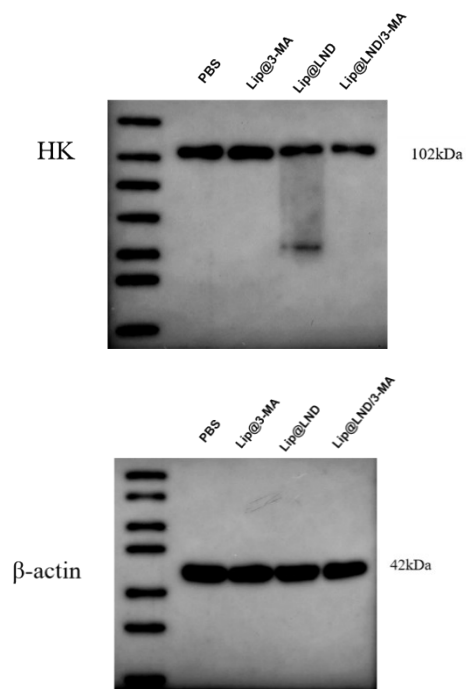


Figure S16. The image of the full gel and blot for Fig 3a.

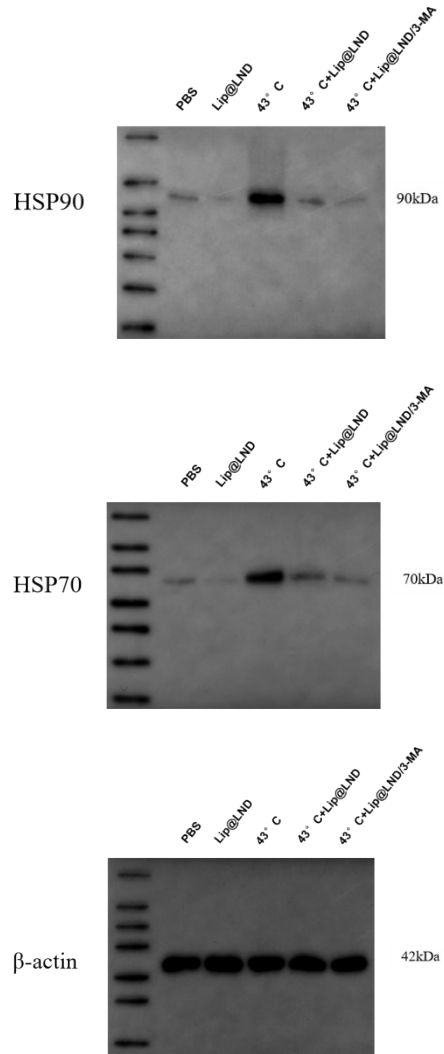


Figure S17. The image of the full gel and blot for Fig 3d.

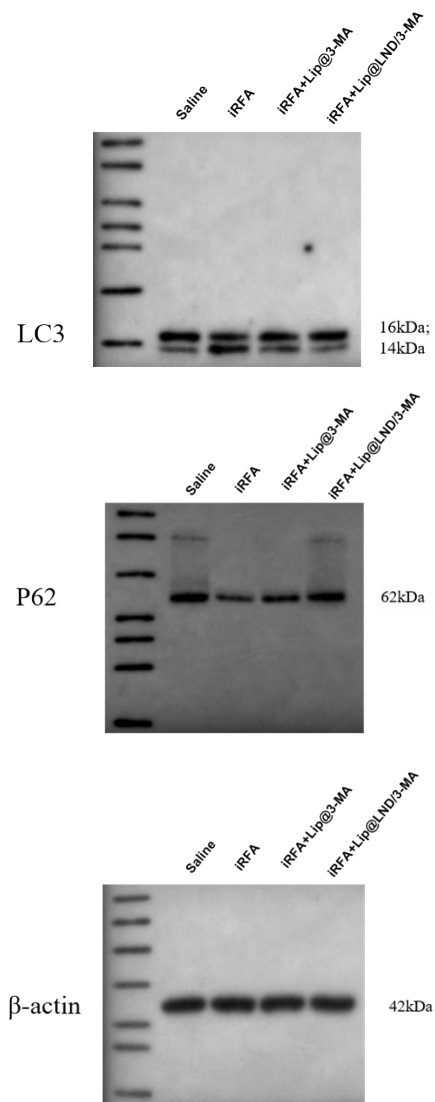


Figure S18. The image of the full gel and blot for Fig 5a.

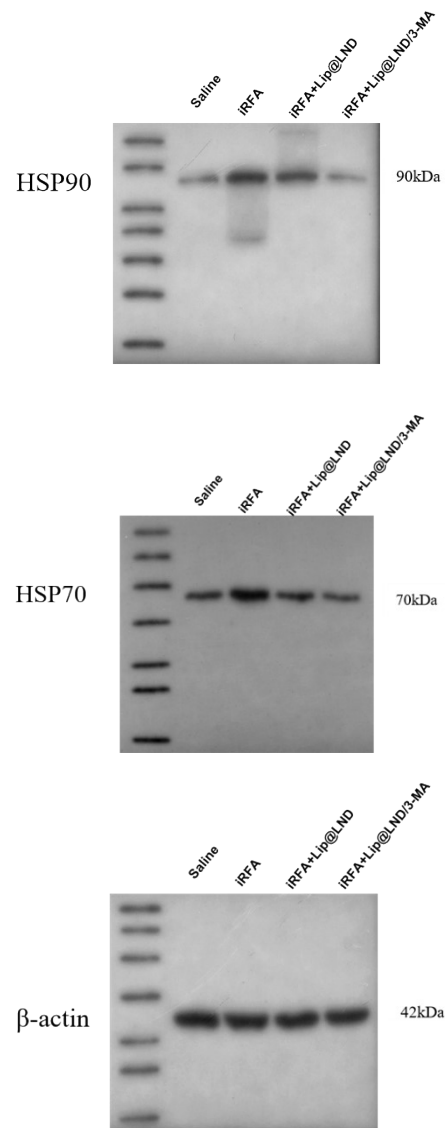


Figure S19. The image of the full gel and blot for Fig 6a.